Nuclear Theory'22
ed. V. Nikolaev, Heron Press, Sofia, 2003

Systematic Study of Structure of ^{12}C-^{22}C

G. Thiamova[1,3], **N. Itagaki**[1], **T. Otsuka**[1,2], **and K. Ikeda**[2]

[1] Department of Physics, University of Tokyo, Hongo, Tokyo 113-0033, Japan

[2] The Institute of Physical and Chemical Research (RIKEN), Wako, Saitama, 351-0198, Japan

[3] Nuclear Physics Institute, Czech Academy of Sciences, Prague-Rez, Czech Republic

Abstract.

The structure of low-lying states of the carbon isotopes is investigated using the Antisymmetrized Molecular Dynamics (AMD) + Generator Coordinate Method (GCM) approach. We can reproduce reasonably well many experimental data for carbon isotopes ^{12}C-^{22}C such as binding energies, the energies of the 2_1^+ states in the even-even isotopes, radii and electromagnetic transition strengths. We investigate the structure change with the increasing neutron number and observe the existence of various exotic phenomena, like the development of neutron skin and large deformations which appear in unstable nuclei. The role of the spin-orbit interaction in the description of the studied isotopes and in the development of cluster structures is discussed. An improved description of the s-orbit is adopted for ^{15}C in an attempt to describe the neutron halo.

1 Introduction

The structure of light neutron-rich carbon nuclei is extensively studied using radioactive isotopes beams. Newly discovered magic number of $N = 16$ corresponds to the driplines of C, N, O isotopes [1,2], namely, the dripline nucleus of the C isotopes is ^{22}C. The nucleus ^{15}C has been known to have the halo structure, due to the valence neutron in the s-orbit.

The situation with another possible candidate for a nucleus with halo structure, namely ^{19}C, is quite controversial. Although several experiments have been

performed to explore the structure of ^{19}C, the ground state spin of ^{19}C still remains unknown. From a simple shell model considerations the valence neutron is expected to occupy the $1d_{5/2}$ orbital. Some shell model calculations suggest a $5/2^+$ ground state with strong contribution from $2s_{1/2}$ neutron coupled to the 2^+ state of ^{18}C at 1.62 MeV [3], others predict a $1/2^+$ as a ground state, while $5/2^+$ is situated at 50-190 keV excitation energy [4, 5]. Study of the Coulomb dissociation of ^{19}C [6] supports the ground state spin $1/2^+$ of this nucleus. If ^{19}C is to be considered as a candidate for neutron halo with the valence neutron in $2s_{1/2}$ orbital, already occupied in ^{15}C, then the natural explanation would be the change of the order of the $2s_{1/2}$ and $1d_{5/2}$ orbitals; while in ^{15}C the former one is lower, the $1d_{5/2}$ orbital becomes lower with increasing neutron number. On the other hand, a lowering of the $2s_{1/2}$ orbital is also possible, in analogy to the ^{11}Be case.

As pointed out in Ref. [7], the ground state of ^{19}C has different predictions from different experimental observables none of which overlaps with each other. The fairly wide tail of the momentum distribution is not successfully interpreted by a model assuming a simple core-plus-$2s_{1/2}$ neutron structure. Recent investigations in GANIL show some indications of the existence of a gamma decay at 200 keV for ^{19}C , from prompt gamma measurements in coincidence with ^{19}C produced by fragmentation [8]. This is the only gamma transition so far observed and it raises the following question. Are there more bound excited states in ^{19}C? If so, an isomeric state might be necessary to explain the GANIL result when no prompt gamma ray other than 200 keV was observed. Further experiments are planned which would search for such an isomeric state.

This is one of the main issues to be understood in C isotopes, together with the change of the order of the $2s_{1/2}$ and $1d_{5/2}$ orbits and mechanism for the appearance of the $N = 16$ neutron magic number. One possible explanation is a structure change in C isotopes where the spin-isospin part of the nucleon-nucleon effective interaction and the p-sd shell interaction play a prominent role [2].

Recent shell-model calculations are another source of information about the structure of the neutron-rich carbon isotopes. Shell model calculations using two types of p-sd Hamiltonian were performed in Ref. [3]: WBT, modeled on a set of two-body matrix elements obtained from a bare G matrix and WBP, modeled on a one-boson exchange potential which includes the one-pion exchange potential and a long range (monopole) interaction. For ^{16}C , WBP gives spectroscopic factors $C^2S(2s_{1/2})$=0.60 and $C^2S(1d_{5/2})$=1.23, and WBT gives $C^2S(2s_{1/2})$=0.78 and $C^2S(1d_{5/2})$=1.07. The spectroscopic factors depend on the single-particle energies and, in particular, on the crossing of the single-particle energies between ^{17}O (where the $1/2^+$ is 0.87 MeV above the $5/2^+$) and ^{15}C. Both WBP and WBT interactions present a triplet of low-lying states for ^{17}C. The WBP interaction gives a $3/2^+$ ground state, in agreement with the

latest experimental results. However, the spectroscopic factors are very similar between WBP and WBT. The $3/2^+$ ground state has basically three components, the main one is $1d_{5/2} \times [(1d^2_{5/2})]_{2^+}$. This accounts for the dominant $l = 2$ knockout to the excited 2^+ state of ^{16}C. The smaller $l = 0$ component to the same state arises from a small admixture of $2s_{1/2} \times [(1d^2_{5/2})]_{2^+}$. The predicted small cross section to the ground state of ^{16}C comes from a small component of $1d_{3/2} \times [(1d^2_{5/2})]_{0^+}$.

The main advantage of the Antisymmetrized Molecular Dynamics (AMD) [9] approach is that it is completely free from any model assumptions such as shell model or clustere structure, axial symmetry of the system and so on. Thus it can describe the system without prejudice. In the light nuclei where both shell model and cluster structure appear the applicability of mean field or cluster models is not assured. The AMD method, on the other hand, can describe both of them easily.

In this paper, we apply the improved version of the Antisymmetrized Molecular Dynamics (AMD) approach and re-analyze the systematics of the C isotopes. The r.m.s. radii, binding and 2^+_1 excitation energies, electric quadrupole moments and the $B(E2, 0^+ \rightarrow 2^+)$ values are calculated and compared with the available experimental data. The agreement between the calculated and experimental data is reasonable. The details of the adopted method and the motivation for its introduction are explained in the next section.

2 Multi-Slater Determinant AMD

The motivation for introducing the improved method is as follows; in previous studies it has been shown that one Slater determinant is not enough to describe a system with developed halo or neutron skin structure. An attempt to improve the description by superposing several Slater determinants did not lead to substantial improvement and the computing time increased considerably.

The improved method which we adopt in this work corresponds basically to the combination of AMD and the Generator Coordinate Method (GCM) [10]. The initial GCM basis wave functions are constructed in such a way that they correspond to a certain value of a properly chosen physical quantity. By changing the value of this quantity, which is constrained during the cooling process, a lot of Slater determinants with different intrinsic structure are prepared. This is much better basis for our AMD calculations.

In this approach the r.m.s. radius is constrained during the cooling process and afterwards a lot of Slater determinants with different intrinsic structure (corresponding to different constrained r.m.s. radii) are superposed. The mixing amplitudes of these Slater determinants are determined after the angular momentum projection by diagonalization of the Hamiltonian matrix. This method can be regarded as a combination of projection after variation (PAV) (the prepa-

ration of the GCM basis by applying the constraint cooling method) and variation after projection (VAP) (GCM diagonalization with angular momentum and parity projected wave functions). We expect that by this double variational procedure more reliable wave functions are obtained than by applying the (PAV) itself. Furthermore, when we solve the cooling equation, different initial sets of parameters are prepared to take into account many local minima of the constraint function, which will be defined later. These minima correspond to different possible geometrical arrangements of the nucleons.

First, we introduce the simple AMD method without any constraint. The total wave function ($|\Psi^{J^\pm}_{MK}>$) is described as a superposition of J^π projected AMD wave functions ($|\Phi^{J^\pm}_{MK}(\boldsymbol{Z}^{n(\beta)};\beta)>$) as follows,

$$|\Psi^{J^\pm}_{MK}(\boldsymbol{Z})>=\sum_\beta c^\beta |\Phi^{J^\pm}_{MK}(\boldsymbol{Z}^\beta;\beta)> . \tag{1}$$

Here β represents the index of an AMD basis function, and the coefficients c^β are determined by diagonalizing the Hamiltonian-matrix. The parameter ($\boldsymbol{Z}$ =$\boldsymbol{Z}_1$,..., $\boldsymbol{Z}_A$) represents the centers of the Gaussian wave packets of nucleons. Here, the parity and the angular momentum are projected to good quantum numbers,

$$|\Phi^\pm(\boldsymbol{Z})>=\hat{P}^J_{MK}\hat{P}^\pm|\Phi(\boldsymbol{Z})>, \tag{2}$$

$$\hat{P}^\pm=\frac{1}{2}(1\pm\hat{P}^{(r)}), \tag{3}$$

$$\hat{P}^J_{MK}=\int d\alpha d(\cos\beta)d\gamma D^{J*}_{MK}(\alpha\beta\gamma)R(\Omega) \tag{4}$$

Each AMD wave function in Eq. (2) for the A-nucleon system has following form:

$$|\Phi(\boldsymbol{Z}_1\boldsymbol{Z}_2,...,\boldsymbol{Z}_A)>=\mathcal{A}[\phi_1\phi_2\cdots\phi_A], \tag{5}$$

$$\phi_i=\psi_i\chi_i, \tag{6}$$

where ϕ_i is the i-th single particle wave function constructed from the spatial part ψ_i and the spin-isospin part χ_i. The spatial part is expressed by a Gaussian wave packet in coordinate representation,

$$\psi_i(\boldsymbol{r})=(\frac{2\nu}{\pi})^{3/4}\exp[-\nu(\boldsymbol{r}-\frac{\boldsymbol{Z}_i}{\sqrt{\nu}})^2+\frac{1}{2}\boldsymbol{Z}_i^2], \tag{7}$$

$$\propto\exp[-\nu(\boldsymbol{r}-\boldsymbol{R}_i)^2+\frac{i}{\hbar}\boldsymbol{K}_i\cdot\boldsymbol{r}], \tag{8}$$

where complex parameters $\boldsymbol{Z}_i$ =$\sqrt{\nu}\boldsymbol{R}_i$+$\frac{i}{2\hbar\sqrt{\nu}}$ $\boldsymbol{K}_i$ represent centers of the Gaussian wave packets and ν is the width parameter, which is fixed to $\nu=\frac{1}{2b^2}$,

$b = 1.6$ fm. In this framework, the AMD wave functions with different intrinsic configurations corresponding to different constrained r.m.s. radii of the total system are superposed.

The diagonal elements of the Hamiltonian-matrix become a function of the parameter $\boldsymbol{Z}$,

$$E(\boldsymbol{Z}, \boldsymbol{Z}^*) \equiv \frac{<\Phi^{\pm}(\boldsymbol{Z})|\hat{H}|\Phi^{\pm}(\boldsymbol{Z})>}{<\Phi^{\pm}(\boldsymbol{Z})|\Phi^{\pm}(\boldsymbol{Z})>}. \tag{9}$$

We optimize these parameters $\boldsymbol{Z}$ before the angular momentum projection by using the frictional cooling method in the AMD,

$$\frac{d\boldsymbol{Z}_i}{d\tau} = -\frac{\partial E}{\partial \boldsymbol{Z}_i^*}, \quad \frac{d\boldsymbol{Z}_i^*}{d\tau} = -\frac{\partial E}{\partial \boldsymbol{Z}_i}. \tag{10}$$

As shown in Ref. [9], by solving this cooling equation, the expectation value of the Hamiltonian (E) decreases as development of the imaginary time τ, since the τ derivative of E is always negative,

$$\frac{dE}{d\tau} = \sum_i^A \frac{\partial E}{\partial \boldsymbol{Z}_i} \cdot \frac{d\boldsymbol{Z}_i}{d\tau} + \sum_i^A \frac{\partial E}{\partial \boldsymbol{Z}_i^*} \cdot \frac{d\boldsymbol{Z}_i^*}{d\tau}, \tag{11}$$

$$= -2\sum_i^A \frac{d\boldsymbol{Z}_i}{d\tau} \cdot \frac{d\boldsymbol{Z}_i^*}{d\tau} < 0. \tag{12}$$

During this optimization of parameters, parity of the system is projected to a good quantum number.

As explained in the beginning of this section one or even several Slater determinants prepared in this way are not enough to describe weakly bound systems. Some of such randomly generated Slater determinants can be basically identical after angular momentum projection.

Now we describe the procedure how to prepare the AMD wave functions with an r.m.s. constraint. First we prepare several initial wave functions by solving a cooling-like equation

$$\frac{d\boldsymbol{Z}_i}{d\tau} = -\frac{\partial f}{\partial \boldsymbol{Z}_i^*}, \quad \frac{d\boldsymbol{Z}_i^*}{d\tau} = -\frac{\partial f}{\partial \boldsymbol{Z}_i}, \tag{13}$$

where the constraint function is

$$f = (O - r_{constr.}^2)^2. \tag{14}$$

Here O is the expectation value of an operator $\hat{O} = \sum_i^A \mathrm{r}_i^2$. The constrained values of the r.m.s. radius, $r_{constr.}$, are shown in Tables 1 and 2. The constraints close to the experimental r.m.s. radius are chosen as these are expected to contribute the most to the binding energy. An important point is that we prepare

Table 1. The number of the employed basis states in the C isotopes as a function of constrained r.m.s. radius (fm). 15 basis states calculated from different initial parameter sets are prepared for each constrained value of the r.m.s. radius.

$r_{constr.}$ (fm)	^{12}C	^{14}C	^{16}C	^{18}C	^{20}C	^{22}C
2.3	15					
2.4	15	15				
2.5	15	15	15			
2.6		15	15	15	15	
2.7			15	15	15	15
2.8				15	15	15
2.9						15

Table 2. The number of the employed basis states for the even-odd C isotopes as a function of constrained r.m.s. radius (fm).

$r_{constr.}$ (fm)	^{13}C	^{15}C	^{17}C	^{19}C	^{21}C
2.3	30				
2.4	30	30			
2.5		30			
2.6			30		
2.7			30	10	
2.8				10	30
2.9				10	30
3.0				10	
3.1				10	
3.2				10	

several wave functions with different initial parameter values for one constrained r.m.s. radius to include many local minima of the constraint function which correspond to different geometrical arrangements of the nucleons having the same r.m.s. radius.

When the value of the constraint function f becomes enough small we proceed to the next step. The initial wave functions correspond in general to highly excited states and are cooled down by solving the frictional cooling equation. The r.m.s. radius is kept constant during the cooling process by introducing a Lagrange multiplier in Eq. (15).

$$\frac{d\boldsymbol{Z}_i}{d\tau} = -\frac{\partial E}{\partial \boldsymbol{Z}_i^*} + \eta \frac{\partial O}{\partial \boldsymbol{Z}_i^*}, \quad \frac{d\boldsymbol{Z}_i^*}{d\tau} = -\frac{\partial E}{\partial \boldsymbol{Z}_i} + \eta \frac{\partial O}{\partial \boldsymbol{Z}_i}, \tag{15}$$

Here, the multiplier η is determined by the condition that the τ derivative of O is zero,

$$\begin{aligned} \frac{\partial O}{\partial \boldsymbol{\tau}} &= \sum_i^A \frac{\partial O}{\partial \boldsymbol{Z}_i} \frac{\partial \boldsymbol{Z}_i}{\partial \boldsymbol{\tau}} + c.c., \\ &= \sum_i^A \frac{\partial O}{\partial \boldsymbol{Z}_i} \{ -\frac{\partial E}{\partial \boldsymbol{Z}_i^*} + \eta \frac{\partial O}{\partial \boldsymbol{Z}_i^*} \} + c.c. = 0. \end{aligned} \tag{16}$$

Therefore, the η value is determined from this equation,

$$\eta = \frac{\sum_i^A \frac{\partial O}{\partial \boldsymbol{Z}_i} \frac{\partial E}{\partial \boldsymbol{Z}_i^*} + c.c.}{\sum_i^A \frac{\partial O}{\partial \boldsymbol{Z}_i} \frac{\partial O}{\partial \boldsymbol{Z}_i^*} + c.c.}. \tag{17}$$

The Hamiltonian and the effective nucleon-nucleon interaction used is the same as in Ref. [11] and the Majorana parameter M of the Volkov No. 2 interaction and the strength of the G3RS spin-orbit interaction are determined by the α-α and α-n scattering phase shift analysis. The strength of the Bartlett and Heisenberg terms of the central interaction has been set to zero.

We want to stress that the study of effective interactions in the AMD model is of importance because it is still not obvious which the effective interaction parameters should be adopted in the AMD framework. The Volkov and modified Volkov interactions, although used in most existing structure AMD studies are not global. Rather some of the parameters have to be optimized for each region of the nuclear mass. In Ref. [12] the Gogny and Skyrme SIII interactions are used to calculate ground state properties of light nuclei. The Gogny force gives in general slightly better results than the SIII force but the tendency is similar for both interactions. Structure of light unstable Li, Be, B and C isotopes using Volkov No.1 and Case(1) and Case (3) of the modified MV1 interactions containing the zero-range three body force as a density dependent term is studied in Ref. [13].

3 Results

The number of basis states employed are summarized in Tables 1 and 2.

In Figure 1 the calculated binding energies are compared with the experimental values. The calculated binding energie of ^{12}C is smaller than the experimental value. It may be partially due to the adopted value of the width parameter ν, which is kept fixed for all isotopes. Since the 3α-like component is important in the ground state wave function of ^{12}C, larger value of ν, closer to the α particle value, could be adopted and the binding energy would increase. To tune the parameter ν to the binding energy is, of course, possible but we would have obtained an effective value of ν, influenced, in general, by the chosen effective interaction and the model space. We will not do it in a systematic way because the Volkov interaction itself is known to give insufficient binding energy for ^{12}C when the Majorana parameter M=0.6, a value adopted to fit the binding energy of ^{16}O. Just for a comparison, when ν=0.21 (b=1.543) is adopted, the ground state binding energy increases aproximately by 2 MeV. Another reason may be stronger spin-orbit term which acts against formation of a cluster structure.

In Figure 2 the energies of the first 2^+ states are shown. A comparison with another AMD calculation [13] with MV1 interaction is done. The calculated 2^+ energy of ^{14}C (8.32 MeV) is higher than the experimental value (7.01 MeV). One of the reasons is most probably larger spin-orbit splitting of the $1p_{1/2}$ and $1p_{3/2}$ spin-orbit partners which brings the dominant proton configuration $(1p_{1/2})^3(1p_{3/2})^1$ higher in energy. Another support for this argument comes also from higher $3/2^-$ state (6.49 MeV) than the experimental value (3.68 MeV) in ^{13}C (Figure 6).

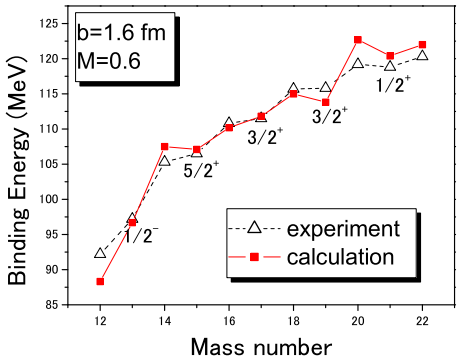

Figure 1. The calculated (squares) and experimental (triangles) binding energies of carbon isotopes.

On the other hand, the spin-orbit interaction plays an important role in describing the 2_1^+ state in ^{12}C. In the cluster model calculations the level spacing between the 0_1^+ and 2_1^+ states was always underestimated. For instance, in a generator-coordinate method (GCM) calculation [14] it was 2.2 MeV, which is much smaller than the experimental value 4.4 MeV. In the present approach this level spacing is well reproduced, and it is because the theory describes the dissociation of the α cluster in the ground state 0_1^+ due to the LS force [15]. Also, in Ref. [13] a systematic study of carbon isotopes is performed, using several sets of effective interactions with much weaker spin-orbit term (900 and 1500 MeV) and the 2_1^+ energies are systematically much smaller than the experimental ones. Thus, it seems that the choice of the proper effective interaction with a spin-orbit term is a key problem in the study of carbon isotopes and needs further investi-

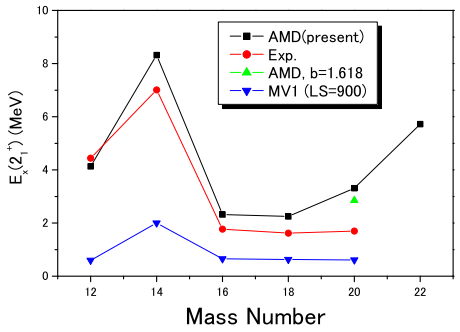

Figure 2. The excitation energies of the 2_1^+ states. The present calculation is represented by squares, circles are the experimental data. Triangles are AMD calculations with modified Volkov interaction MV1 containing zero range density dependent term.

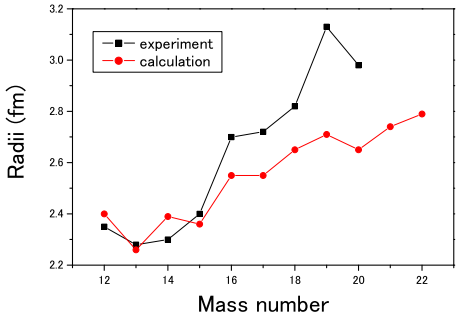

Figure 3. Calculated (circles) and experimental (squares) r.m.s. radii, deduced from interaction cross sections by Glauber model.

gation.

The overbinding observed for ^{20}C and ^{22}C can be also partially related to the used spin-orbit interaction. Furthermore, we observe an increase of the 2_1^+ energy in ^{20}C. Our calculation thus suggests a $(1d_{5/2})^6$ sub-shell closure, not observed in the experimental data. On the contrary, the experimental values of the 2_1^+ energies of ^{16}C, ^{18}C and ^{20}C are almost the same, suggesting the $2s_{1/2}$ and $1d_{5/2}$ orbits are almost degenerate in these isotopes. In our case, the large spin-orbit splitting of the $1d_{5/2}$ and $1d_{3/2}$ orbits brings the $1d5/2$ orbit lower in energy and the sub-shell closure may develop. This effect may be partially responsible for the fact, that the calculated spin of the ground state of ^{15}C is $5/2^+$ instead of $1/2^+$, as is shown later. Another contribution may come from the width parameter ν and the Majorana parameter M. Smaller ν and larger M could be adopted when going to heavier isotopes, which would give somewhat smaller binding energies.

Although the calculated values of the r.m.s. radii are relatively smaller than the experimental ones (see Figure 3), both show drastic increase at ^{16}C. This kink of the r.m.s. radius is mainly due to the fact that two valence neutrons are added to the sd-shell. The radii are known to be sensitive to the value of the Majorana parameter M. Larger values of M can be adopted for heavier isotopes which would lead to slightly larger radii. In our calculations this parameter has been kept constant ($M = 0.6$) over the whole isotope region for the sake of simplicity. We expect that systematically larger radii can be obtained when a density dependent interaction is used because r.m.s. radii are also sensitively dependent on it. The radii become larger and larger in the region heavier than ^{14}C. This is mainly due to the fact that the neutron radii become larger due to the development of the neutron skin structure (another evidence comes from the neutron quadrupole moments, as shown later) while the proton radii are more stable with the increase of the neutron number, similarly to the results in Ref. [13].

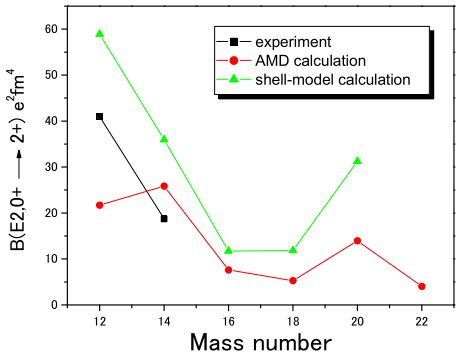

Figure 4. B(E2) transitions; circles are the present calculations, triangles are the shell-model calculations and squares are the experimental data.

In Figure 4 the $B(E2)$ values are presented. The calculated $B(E2)$ value for ^{12}C is smaller than the experimental value. We expect that by increasing the amplitude of the 3α component of the ground state wave function it will become larger. The $B(E2)$ values for the ^{16}C and ^{18}C isotopes are very small. As is discussed in Ref. [17] the neutron effective charges become very small in the nuclei where the neutrons are weakly bound. In ^{16}C almost all contribution to the $B(E2)$ value comes from the neutrons because protons construct almost closed shell model configuration. Thus the reduction of the neutron effective charges affects the $B(E2)$ value strongly. Namely, the reduction of the neutron effective charge for the transition between the $2s_{1/2}$ and $1d_{5/2}$ orbits is of importance, because the ground state of ^{16}C contains a large $(2s_{1/2})^2(\nu)$ component. The similar mechanism makes the $B(E2)$ value small for ^{18}C. The B(E2) value for ^{16}C has been measured recently [18] and it is indeed very small. In ^{20}C the proton contribution to the $B(E2)$ values becomes again larger, because the contribution of protons increases. In general, we can say, that the results we have obtained within the AMD method with bare charges are in qualitative agreement with the above mentioned shell model calculations. Although our $B(E2)$ values are smaller that those in Ref. [17] the tendency seems to be reproduced by our model.

The quadrupole moment of protons Q_p of ^{16}C is much smaller than Q_n, as should be expected for a closed shell proton configuration (Figure 5). The same is truth also for ^{18}C. Slight increase of Q_p is observed in ^{20}C. The quadrupole moments Q_p and Q_n are almost the same in ^{12}C, while Q_n decreases significantly in ^{14}C with the neutron magic number $N = 8$. Again, we would expect larger values for ^{12}C if the 3α component were stronger in the ground state wave function. We may notice much larger absolute values of the neutron quadrupole moments than the protons ones in the neutron-rich region, which shows that the

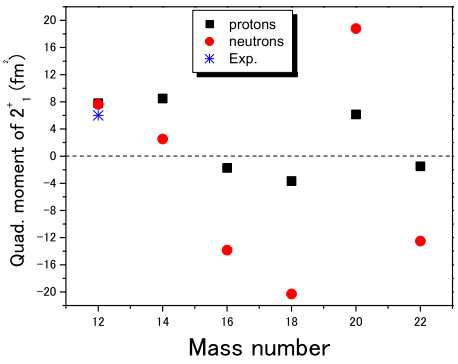

Figure 5. Quadrupole moments of protons (squares) and neutrons (circles).

neutron density in the neutron-rich region stretches widely in outer region. We would like also to remind that in Ref. [19] where the Skyrme SIII case interaction is employed in an AMD calculation without angular momentum projection the proton deformation of ^{16}C and ^{18}C is prolate, similar to our case. Protons of these nuclei then would be separated into two spatial parts. On one side, there are two protons, and on the other side, there are four protons. The Hartree-Fock calculations with the Gogny force [20] and with the Skyrme SIII force [21] also give prolate proton deformations for ^{16}C and ^{18}C. However, the results of the AMD calculation with the MV1 force [22] contradict these results, suggesting, that protons of the carbon isotopes are all oblately deformed. From all these results it seems that the proton deformation of ^{16}C and ^{18}C is more sensitive to the effective interaction. We would like to stress another interesting feature observed in our calculation, namely that the proton distribution seems to adjust its deformation to the neutron one, to increase the overlap of the proton and neutron matter distribution. This may show the importance of the proton-neutron interaction in neutron-rich nuclei.

Next we discuss the even-odd C isotopes in more detail.

As seen from Figure 1, the ground state spins of ^{15}C and the halo structure of ^{19}C nuclei are not reproduced. However, we have to remind us, that the ground state properties of ^{19}C are not very well know experimentally. It is possible that the large interaction cross section from which the large r.m.s. radius has been extracted is due to the presence of an isomeric state as suggested by the measurements in GANIL [8].

In ^{15}C the $2s_{1/2}$ orbital is below the $1d_{5/2}$ orbital. This fact is clearly observed as an abnormal ground state spin parity $J^\pi = 1/2^+$ of this nucleus. The lowering of the s orbital is due to the halo formation. The halo is formed since the orbital with lowest angular momentum gains energy by extending the wave function. For ^{15}C we did not obtain the ground state spin $1/2^+$. Our calcula-

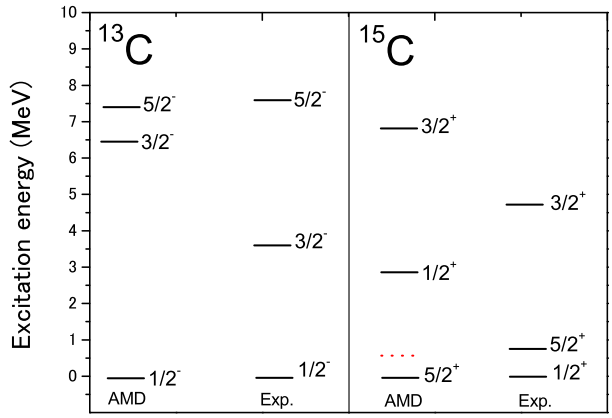

Figure 6. The excitation energies of the $1/2^+$, $3/2^+$ and $5/2^+$ states. The dotted line represents the excitation energy of $1/2^+$ when angular momentum projection + multiple relative orientation (between the core and neutron) is adopted.

tion gives -104.2 MeV for the $1/2^+$ state and -107.1 MeV for the $5/2^+$ state (Figure 6). The fact that the $5/2^+$ state is lowest may be also given by stronger spin-orbit interaction which brings the $1d_{5/2}$ orbit down in energy. Another indication of a stronger spin-orbit term comes from overestimated excitation energy of the first $J^\pi = 3/2^-$ state in ^{13}C (Figure 6). In Ref. [9], where the MV1 force with density dependent term is used to calculate the magnetic moments of the carbon isotopes the ground state spin $1/2^+$ of ^{15}C is not reproduced either. This may also show the limitation of the AMD approach which may be too simple for the description of the exotic, neutron-rich nuclei.

To describe the tail of the wave function we have to express better the s-orbit. If we only project the total J^π of ^{15}C, the wave function describing the relative motion of the valence neutron and ^{14}C is not optimized, and we cannot obtain correct ordering of the levels. Therefore, a different approach is necessary, especially for the weakly bound systems with deformed cores. We express this effect by superposing single projected wave functions. First, the core wave functions (^{14}C) are generated and afterwards on each of them several wave functions of the last valence neutron are superposed. If the basis states of ^{14}C correspond to the r.m.s. constraint 2.3, 2.4 and 2.5 fm (only one basis state for each r.m.s. radius) and for each of them 16 basis states for the odd neutron corresponding to different relative orientations relative to the core are superposed, the $1/2^+$ is still about 1 MeV higher than $5/2^+$, which is, however much less than without the double projection where this energy difference is typically several MeV. When a larger number of basis wave functions is adopted (5 wave functions for 3 dif-

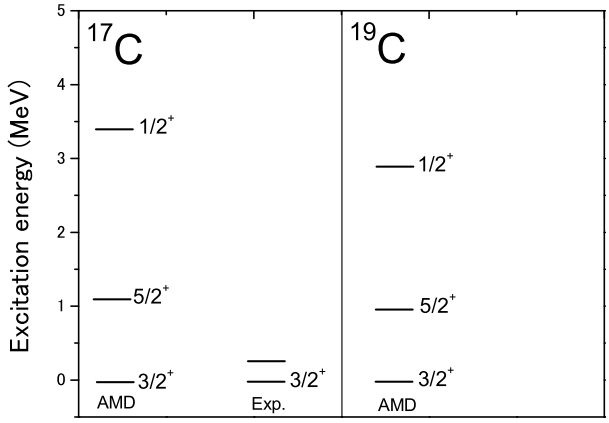

Figure 7. The excitation energies of the $1/2^+$, $3/2^+$ and $5/2^+$ states.

ferent r.m.s. constraints for ^{14}C and for each of them 10 wave functions for the valence neutron) the $1/2^+$ state is 0.6 MeV above $5/2^+$ (see dotted line on the right panel of Figure 6).

The low-lying levels of ^{17}C and ^{19}C are shown in Figure 7. The latest experiments favor ground state spin $J = 3/2^+$ for ^{17}C [23], which is reproduced by our calculation. In case of ^{19}C the basis states with large r.m.s. radii are employed in an attempt to reproduce the suggested large r.m.s. radius. The obtained energies are -110.9 MeV, -113.8 MeV, and -112.8 MeV for the $1/2^+$, $3/2^+$, and $5/2^+$ states, respectively. In general, in all calculations we have performed (with different number of basis wave functions, r.m.s. constraints, strength of the spin-orbit interaction) the energies of the first $1/2^+$, $3/2^+$ and $5/2^+$ states are close to each other and in some of them the $5/2^+$ state is lowest. The variation of the spin-orbit strength affects also the $1/2^+$ which shows that this state has a Nilsson-like character in this model. We should remind us that similar results have been obtained also in Ref. [3], where shell model calculations led to a triplet of low-lying levels with spin-parity $1/2^+$, $3/2^+$ and $5/2^+$ and their ordering depended on the adopted effective interaction, similarly to ^{17}C. It is considered that the $1/2^+$ state can be pulled down by the same approach as has been done for ^{15}C. We can conclude that the idea of a valence neutron in s-orbit used to explain the large r.m.s. radius of ^{19}C is not supported by our calculation.

In general, the strongly attractive $1p_{1/2}(\pi)$-$1d_{5/2}(\nu)$ central and tensor interactions [2], would be partially responsible for the crossing of the $1d_{5/2}$ and $2s_{1/2}$ orbits in the carbon isotopes. This effect is not fully included in our model. Another contribution would come from the pairing interaction between neutrons on the $1d_{5/2}$ orbital. Such effects are probably not well described by our interac-

tion. On the other hand, the lowering of the $2s_{1/2}$ single particle energy coming from the decrease of the kinetic energy can be taken into account in our method, as done for ^{15}C. However, as has been stressed at the beginning, the situation with the ground state of ^{19}C is still unclear and awaits further experimental investigations.

4 Conclusion

In this paper we have presented systematic calculations for ^{12}C-^{22}C. Large number of quantities have been calculated for the even-even isotopes. The calculated binding energies are in reasonable agreement with the experimental data. The systematic comparison of the binding and 2_1^+ energies of the even-even isotopes with the experimental data reveals the importance of the spin-orbit term of the effective interaction. Specifically, the calculated energy of the 2_1^+ state in ^{14}C and the observed sub-shell closure in ^{20}C suggest the spin-orbit term should be weaker. On the other hand, with weaker spin-orbit interaction the energy of the 2_1^+ state in ^{12}C is much lower than the experimental value. It seems that this point deserves further detailed investigation. It will be possible to make more conclusive statements concerning the effective interaction when even larger model space is used.

The neutron magic number $N = 8$ is reflected by the large 2_1^+ energy of ^{14}C. Very large 2_1^+ energy of ^{20}C supports the idea of $N = 16$ neutron magic number.

The r.m.s radii systematically increase beyond ^{14}C. It can be explained by the development of the neutron skin. This fact is reflected also by the neutron quadrupole moments, which increase beyond ^{14}C, indicating the neutron matter distribution stretches widely in outer region. An interesting tendency is observed in the behaviour of the proton deformation which seems to adapt to the neutron one.

The calculated $B(E2)$ values show good tendency, similar to this obtained by shell model calculations with reduced effective neutron charges. The advantage of the AMD method is that no effective charges have to be used, because the changes of neutron and proton distribution are authomatically described by the model. Recently measured very small $B(E2)$ value for ^{16}C is successfully reproduced by our model.

The calculated binding energies for the even-odd isotopes are in good agreement with the experimental values. The ground state spin of ^{17}C is reproduced. In case of the ^{15}C isotope good description of the tail of the wave function is important. When the s-orbit is expressed properly a much lower $1/2^+$ state is obtained. The situation with the ground state spin of ^{19}C is unclear and further experiments are necesssary to solve the controversial predictions from the previous experiments.

Acknowledgement

One of the authors (N.I.) thanks Prof. H. Horiuchi, and Dr. Y. Kanada-En'yo for fruitful discussions. This work is supported in part by Grant-in-Aid for Scientific Research (13740145) from the Ministry of Education, Science and Culture. The financial support from the Japanese Society for Promotion of Science under grant No. Po 1769 is acknowledged.

References

[1] A. Ozawa, T. Kobayashi, T. Suzuki, K. Yoshida, and I. Tanihata (2000) *Phys. Rev. Lett.* **84** 5493.

[2] T. Otsuka, R. Fujimoto, Y. Utsuno, B. A. Brown, M. Honma, and T. Mizusaki (2001) *Phys. Rev. Lett.* **87** 082502.

[3] V. Maddalena *et al.* (2001) *Phys. Rev. C* **63** 024613.

[4] D. Bazin *et al.* (1995) *Phys. Rev. Lett.* **74** 3569.

[5] E. K. Warburton and B. A. Brown (1992) *Phys. Rev. C* **46** 923.

[6] T. Nakamura *et al.* (1999) *Phys. Rev. Lett.* **83**, 1112

[7] R. Kanungo *et al.* (2000) *Nucl. Phys. A* **677**, 171

[8] GANIL, *private comunication*.

[9] Y. Kanada-En'yo and H. Horiuchi (1996) *Phys. Rev. C* **54** R468.

[10] N. Itagaki and S. Aoyama (2000) *Phys. Rev. C* **61** 024303.

[11] N. Itagaki and S. Okabe (2000) *Phys. Rev. C* **61** 044306.

[12] Y. Sugawa, M. Kimura and H. Horiuchi (2001) *Prog. Theor. Phys. Suppl.* **106** 1129.

[13] Y. Kanada-En'yo and H. Horiuchi (2001) *Prog. Theor. Phys. Suppl.* **142** 205.

[14] E. Uegaki, S. Okabe, Y. Abe and H. Tanaka (1977) *Prog. Theor. Phys.* **57** 1262; E. Uegaki, Y. Abe, S. Okabe and H. Tanaka (1978) *Prog. Theor. Phys.* **59** 1031; (1979) **62** 1621.

[15] Y. Kanada-En'yo (1998) *Phys. Rev. Lett.* **81** 5291.

[16] A. Ozawa, T. Suzuki, and I. Tanihata (2001) *Nucl. Phys.* **A 693** 33.

[17] R. Fujimoto (2002) *PhD thesis*, University of Tokyo.

[18] N. Imai and Z. Elekes *private communication*.

[19] M. Kimura, Y. Sugawa and H. Horiuchi (2001) *Prog. Theor. Phys.* **106** 1153.

[20] R. Blumel and K. Dietrich (1987) *Nucl. Phys. A* **471** 453.

[21] N. Tajima, S. Takahara and N. Onishi (1996) *Nucl. Phys. A* **603** 23.

[22] Y. Kanada-En'yo, H. Horiuchi and A. Ono (1995) *Phys. Rev. C* **52** 628.

[23] K. Asahi *et al.* (2002) *Nucl. Phys. A* **704** 88c.